www.sciencetranslationalmedicine.org/cgi/content/full/6/238/238ra69/DC1

Supplementary Materials for

Photoactivation of Endogenous Latent Transforming Growth Factor–β1 Directs Dental Stem Cell Differentiation for Regeneration

Praveen R. Arany, Andrew Cho, Tristan D. Hunt, Gursimran Sidhu, Kyungsup Shin, Eason Hahm, George X. Huang, James Weaver, Aaron Chih-Hao Chen, Bonnie L. Padwa, Michael R. Hamblin, Mary Helen Barcellos-Hoff, Ashok B. Kulkarni, David J. Mooney*

*Corresponding author. E-mail: mooneyd@seas.harvard.edu

Published 28 May 2014, *Sci. Transl. Med.* **6**, 238ra69 (2014)
DOI: 10.1126/scitranslmed.3008234

The PDF file includes:

Materials and Methods

Detecting ROS in a cell-free system

Fetal bovine serum (FBS; Gibco, Life Technologies) was diluted in molecular grade water (G Biosciences) and subjected to LPL treatments at various fluences or treatment with specific ROS-generating reagents (table S1). The solutions were then immediately incubated with the following fluorescent dyes to assess specific ROS; MitoSOX Red (5 μM) for superoxide, Amplex UltraRed (50 μM) for H_2O_2, and proxyl fluorescamine (100 μM) for hydroxyl radicals (all from Molecular Probes, Life Technologies). The Amplex UltraRed assay was performed in the presence of horseradish peroxidase (0.2 U/ml). Fluorescence was assessed with a microplate reader (Synergy HT, Bio-Tek Instruments) and concentrations were estimated from a standard curve in each assay. In some experiments, pre-incubations with a ROS scavenger, NAC (1 mM) (Sigma), for 30 min prior to LPL treatments were performed. ROS probes were added immediately after the 5-min LPL treatments, to avoid the probe acting as photosensitizers themselves, and incubated for 25-30 min for individual probes at room temperature as per manufacturer's instructions. In some experiments, deuterium (Sigma) was used instead of water to dilute serum while in other assays, FBS was incubated with Chelex 100 resin (Biorad) overnight as per manufacturer's instructions, and centrifuged to remove beads before use.

Free cysteine assay

We developed an assay to assess how LPL affected protein conformation change based on exposed cysteines. A fluorescent dye, 5-[(2-[(iodoacetyl) amino] ethyl) amino] naphthalene-1-sulfonic acid (IAEDANS) (Molecular Probes, Life Technologies) was used that produces a spectral shift with a

strong fluorescence signal (ex/em 336/490 nm; extinction coefficient 5700) when bound to free thiols. Solutions were incubated with the IAEDANS dye and assessed for an increase in fluorescence with a microplate reader. The IAEDANS tagged complexes were separated by gel electrophoresis, under native or reducing conditions, in 1D (based on charge: mass) or 2D format (based on isoelectric points and then, charge:mass. Tagged complexes could be identified by western blotting, either native or reducing depending on potential complexes, or by using a high-throughput screening approaches such as mass spectroscopy.

For experiments, fetal bovine serum (70%) or latent TGF-β1 (1 μg/ml) (R&D Systems) solutions were irradiated with LPL at 3 J/cm^2 and incubated with IAEDANS dye (250 μM) at 37^{o}C for 30 min. Fluorescence was measured with a microplate reader (Synergy HT and KC4 software, Bio-Tek Instruments). These solutions were separated on an SDS reducing polyacrylamide gradient gel (4-20% Tris-Glycine PAGE, Life Technologies), visualized on a UV transilluminator (365 nm, Hoefer) and stained with Coomassie Blue (G250) (Eastman Chemical) for total protein. Some gels were transferred to a nitrocellulose membrane and subjected to western blotting for TGF-β.

Bradford assay

Samples were subjected to a modified Bradford assay to estimate total protein as per manufacturer's instructions (BCA, Thermo Scientific Inc). Absorbance was measured at 560 nm with a microplate reader (Synergy HT and KC4 software, Bio-Tek Instruments).

Semi-quantitative RT-PCR

At 7 days, cells were washed with PBS, lysed in Trizol (Life Technologies) and total RNA was extracted with the RNeasy Mini kit (Qiagen). RNA was reverse-transcribed by using SuperScript III RT-PCR system (Life Technologies) according to the manufacturer's protocol. One microliter of cDNA sample was amplified by PCR for specific genes representing dentin matrix (table S2). Images were scanned digitally, inverted (to black bands on white background), brightness and contrast were adjusted for the whole image wherever appropriate.

ELISA

TGF-β1 was measured with an ELISA (Promega) performed as per the manufacturer's instructions. Briefly, solutions were incubated in microplate wells coated with the anti-TGF-β1 monoclonal capture antibody that only binds to physiologically active TGF-β1 dimer capable of binding its receptor but not LTGF-β1. This was followed by the secondary antibody and detection with a colorimetric substrate. Absorbance was read on a microplate reader (Synergy HT and KC4 software, Bio-Tek Instruments). To assess total (activatable) TGF-β1 in these samples, an aliquot of the sample is subjected to chemical treatment namely, 1 N HCl 1:50 v/v for 10 min followed by 1.2 N NaOH with 0.5 M HEPES 1:50 v/v to neutralize for 10 min (all from Sigma) prior to assessment in the assay.

Generation and characterization of conditional knockout (*DSPP*^{Cre}*TGF-βRII*$^{fl/fl}$) mice

DSPP^{Cre} mice were bred with *TGF*-β*RII*$^{fl/fl}$ mice to generate *DSPP*^{Cre}*TGF*-β*RII*$^{fl/fl}$ mice. The transgenic construct consists of a 6 kbp upstream regulatory sequence of *DSPP* fused to 1.6-kbp Cre recombinase with a nuclear localization sequence, and a 500-bp SV40 polyadenylation sequence. To confirm the *TGF*-β*RII* deletion in the teeth of the conditional KO (coKO) mice, PCR was performed using tail

genomic DNA as well as tooth DNA. PCR primers and conditions are listed in table S2. Subsequently, the *DSPP*^{Cr} and *TGF*-β*RII*$^{fl/+}$ heterozygous mice were crossed with other *TGF*-β*RII*$^{fl/fl}$ mice to generate coKO mice. These mice have a mixed strain background of C57B6/129SVJ/FvBN. Skulls from 2 month-old coKO and fl/fl control animals were harvested, cut in two pieces symmetrically and fixed in 4% PFA overnight. The skulls were then washed in phosphate buffer saline (PBS) and radiographed (Faxitron Biooptics). Microcomputed tomography (μCT) and histological analyses were performed on dissected mice teeth as described in methods section.

To confirm Cre expression in coKO mice, 2 day–old coKO and *TGF*-β*RII*$^{fl/fl}$ mouse skulls were fixed with 4% PFA overnight and decalcified for 2 weeks in 0.1-M EDTA solutions. Cross-sections of decalcified molars were cut from paraffin blocks at 6-μm thickness and placed onto slides. Slides were deparaffinized using xylene and gradually hydrated through 100%, 95%, and 70% ethanol and water. Quenching of endogenous peroxidase activity was performed by incubating the sections in 6% H_2O_2 in TBST (Tris-buffered solution with Tween) for 10 min. Sections were then incubated for 1 h in blocking solution and then incubated with primary antibodies against Cre (table S3) diluted in TBST/1% BSA and applied to the slides and incubated for two hours at room temperature. Slides were then incubated with the biotinylated secondary antibody for 30 min followed by the Vectastain Elite ABC reagent (Vector labs) for 30 min, washed 3 times for 5 min each in TBST and incubated in DAB developing solution. Counterstaining with hematoxylin was performed and mounted for histological analyses.

PLG microsphere synthesis and release

Poly(lactide-*co*-glycolide) (PLG) (8515DLG7E, Lakeshore Biomaterials) microspheres containing SB431542 were prepared by a solvent evaporation method using a double emulsion technique. Briefly,

100 µl of proteins dissolved in molecular grade water were pipetted into 1 ml of 5% PLG in ethyl acetate (Sigma) and immediately sonicated (Sonics) for 1 min. The second emulsion composed of 1% polyvinyl acetate (Sigma) and 7% ethyl acetate was then added and vortexed for 15 s and finally added to a 1% polyvinyl alcohol (Sigma) solution with continuous stirring for 3 hours at room temperature. The solutions were then filtered through a 0.2-µm filter (Nalgene), collected by centrifugation at 2000 rpm for 10 min (Eppendorf), freeze-dried for 16 h (Labconco), and stored at -20^{o}C. To assess inhibitor release, microspheres were suspended in PBS with 0.05% sodium lauryl sulfate in microfuge tubes (Eppendorf) in a 37^{o}C incubator on a rotator. At given time intervals, solutions were centrifuged and supernatant was collected for liquid chromatography–mass spectrometry (LC-MS) analyses.

LC-MS

LC-MS studies were carried out with a 1290 Infinity LC interfaced with the 6140 Quadrupole MSD system (both Agilent Technologies). The MS instrument was calibrated with NaI/CsI solution infused into the ESI interface using the automated tuning and a built-in calibrant delivery system. Samples were analyzed using the reverse-phase X Bridge C18 column (3.5 µm particle size, 4.6×150 mm internal diameter and length) (Waters). The solvents 0.1% ammonium hydroxide in water (Solvent A) and 0.1% ammonium hydroxide in acetonitrile (Solvent B) were used at a flow rate of 1 ml/min, 5% B was held for 0.25 min, followed by a gradient over 9.5 min to 100% B which was held for 0.44 min and column was returned to initial conditions for 0.06 min at 5% B. Samples were monitored using UV (210 and 254 nm), and selective ion monitoring (SIM) of m/z 385 in ES positive mode. Using the SIM signal, a standard curve of serially diluted SB431542 (Calbiochem) in methanol (HPLC grade, Baxter) was created and used for quantitation. The SIM chromatograms were integrated with LC-MSD Chemstation Software (Rev. B.04.02, Agilent Technologies).

PLG scaffold fabrication

Macroporous PLG scaffolds were fabricated with a gas foaming - salt leaching technique. Briefly, PLG (8 mg) (85:15, 120 kDa copolymer, Alkermes) was mixed with the porogen, sodium chloride (Sigma, 150 mg, ground and sieved to particle size between 250 and 425 µm) and compression molded. The resulting disc was allowed to equilibrate within a high-pressure CO_2 environment, and a rapid reduction in pressure causes the polymer particles to expand and fuse into an interconnected scaffold structure. Salt was then leached from the scaffolds by immersion in water, yielding scaffolds that were 90% porous. These were sterilized with 70% ethanol, serum-coated overnight, and cells were seeded for various experiments.

Luciferase reporter assay

MvLu1 cells were stably transfected with the promoter of the TGF-β responsive gene, *plasminogen activator inhibitor* (*PAI*), which is tagged to luciferase (p3TP luc) (kind gift from D. Rifkin). This reporter assay was used to assess activation of TGF-β signal transduction in 2D and 3D cultures following LPL treatments described below. These cells are known to be exquisitely sensitive to TGF-β inhibition and hence, assaying cell density and normalization of luciferase activity to total protein is critical.

Reporter assays in 2D. Mv1Lu cells were plated in a 24-well plate (40,000 cells/well) (Nunc, Thermo Fisher Scientific) in complete media. After 4 hours, LPL irradiation at 3 J/cm^2 or recombinant TGF-β1 (2.5 ng/ml) treatment in 0.2% FBS were performed. Some well were pretreated with NAC (1 mM) or SB431542 (10 µM) prior to LPL irradiation. Cells were lysed at 24 h in passive lysis buffer

and luciferin substrate (both Promega) was added to evaluate luciferase activity with a microplate reader.

Reporter assays in 3D. PLG scaffolds were fabricated as described previously and MvLu1 cells were seeded onto them (3×10^6 cells / ml) in complete media. Cells were allowed to attach for 30 min and scaffolds were then floated in complete media. After 4 h, LPL irradiation or TGF-β1 treatment were performed. Some scaffolds were pre-incubated with NAC (1 mM) prior to LPL irradiation. Scaffolds were replaced in the incubator overnight. The following day, scaffolds were washed briefly in PBS, and coelenterazine (25 µg/ml) (Nanolight Technology) was added to evaluate luciferase activity with a bioluminescence imaging system (Xenogen, Caliper Life Science). Further, to quantitatively assess luciferase expression, scaffolds were subsequently washed in PBS, lysed in passive lysis buffer (Promega) and assayed in a microplate reader as described above.

Ultra-structural analyses of mineralized tissue

Tooth specimens were processed and the spatial distribution of organic and inorganic components was determined using Raman mapping. Briefly, extracted teeth were cleaned and dehydrated in ethanol, infiltrated, and embedded without demineralization in methyl methacrylate. Non-decalcified sections (10 µm thick) were cut with a Leica RM 2165 microtome. The specimens were further manually polished under water with 600 grit SiC paper. A Raman microscope (Senterra, Bruker) with a 785 nm laser operating at 50 mW was used to collect Raman spectra and images. It was built on an Olympus BX51 microscope, a motorized XYZ stage with a minimum step width of 100 nm, and a TE-cooled (-70^{o}C) CCD camera with 1024×256 pixels. Raman imaging with the following parameters was used: 400 lines/mm grating, 140-µm confocal hole, 100-µm slit width, and a 20X objective; spectra were obtained from 90 to 3500 cm^{-1} and with a 20-second integration time. Without additional spectral

smoothing, the individual spectra were adjusted using multiple-point baseline correction (concave rubber band correction) and mapping spectra for imaging were adjusted using polynomial baseline correction.

Representative Raman spectra from enamel, dentin, cementum and bone were obtained (fig. S2A). LPL-induced pulpal mineralization was compared to the characteristic Raman peaks of the tertiary dentin induced by calcium hydroxide, based on the ratios of CH at 1450 cm^{-1} to ν1 of PO_4^{3-} at 960 cm^{-1} (fig. S2B). For Scanning Electron Microscopy and Energy Dispersive X-ray spectrometry (SEM-EDS), samples were sputter-coated with platinum-palladium and assessed for mineral content (calcium, phosphate, oxygen over carbon weight percentage) with SEM-EDS (Evo-55, Carl Zeiss). For the polychromatic SEM imaging, a Tescan instrument at 20 kV with multiple secondary electron detectors was used and sample images were pseudo-colored color based on variability in surface slopes.

Microcomputed tomography (μCT) imaging

Extracted rodent tooth specimens were individually analyzed for tertiary dentin induction using a μCT instrument (X-Tek, Nikon Meteorology Inc). Image frame rates were optimized based on the sample size ranging from 2900 to 3300 frames. A CCD panel detector (Perkin-Elmer) with 2000 × 2000 pixels, 7.5 frames per second, and pixel size of 200 μm was used to capture and reconstruct images with imaging software (Inspect-X and CT-Pro, Nikon Meteorology Inc). Standardization of two x-ray sources, voltage, current and exposure times were performed. The transmission source was noted to

provide significantly better contrast and resolution compared to a reflected power source due to its smaller spot size. The transmission source was chosen to perform the rest of the analyses. Samples were scanned at 90 kV, 90 µA with a 4-second exposure time per frame that provides a 3.6 µm voxel resolution. For an average of 3000 frames per sample, each scan took about 3.5 hours. This methodology was particularly important to facilitate the sensitive assessment of newly (lower) mineralized tertiary dentin allowing segmentation from surrounding, normal (slightly higher) mineralized dentin. Given the large volume of the defect created by pulp exposure in the relatively small rodent teeth, the complete 3D CT image was chosen for analyses.

Image analysis was performed with VG Studiomax v2.0 (Volume Graphics). Image analyses were carried out to first segment out the enamel, cement, or other exogenous debris, and then the software used a surface and pixel (mineral) density algorithm to assess dentin. The segmented dentin selected by this process was visually confirmed in all three axes and any discernible bone or non-dentin materials infrequently highlighted during segmentation were manually excluded. The 3D reconstructed sample was then subjected to volumetric analyses represented as a ratio of the bone (dentin) volume over total volume (BV/TV).

Alkaline phosphatase (ALP) assay

Cells were lysed in lysis buffer (50 mM Tris HCL and 0.1% Triton X 100, pH 9.5, both Sigma) and 10 µl lysate was incubated with 100 µl of 4-MUP substrate (Sigma) at 37^{o}C for 30 min. Fluorescence was assessed with a microplate reader and normalized to total protein.

In vivo imaging for inflammation

Anesthetized mice were subjected to two pulp exposures in their maxillary molars. One site was treated with a low power laser (810 nm, GaAlAs) for 5 min for total fluence of 3 J/cm^2 and restorations were placed on both sites. After 24 hours, mice were placed under general anesthesia in an induction chamber with 4% isoflurane via a calibrated vaporizer connected to a gas evacuation unit. Mice were injected with the inflammation detection probe (XenoLight RediJect, PerkinElmer, 200 mg/kg, 100 µl per mice, i.p.) 5 min prior to imaging, placed in the IVIS Lumina XR imaging station and fluorescence images were acquired with the Living Image software (Perkin-Elmer).

Supplementary Figures

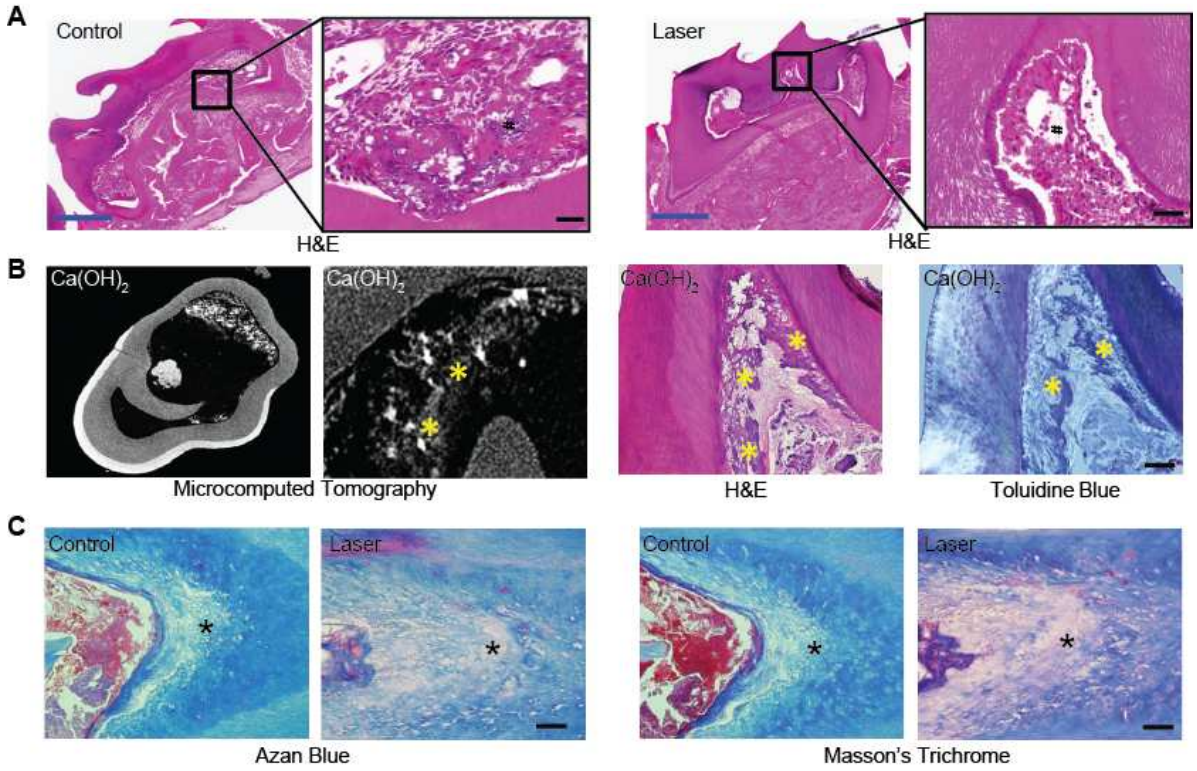

Fig. S1. Characterization of tertiary dentin induction by histology and µCT. (**A**) H&E-stained sections of decalcified rat teeth at low (left) and high (right) magnification to examine inflammatory (round) cell infiltrate in either no treatment (Control) or LPL treatment (Laser). Tissue damage / cement restoration ($^{\#}$) were used to identify areas directly exposed by tooth drilling. Scale bars, 500µm (blue) and 200 µm (black). (**B**) As positive controls for tertiary dentin induction, calcium hydroxide dressing was placed on the exposed pulp. µCT (left) and histology (right) imaging of rat teeth was performed at 12 weeks to assess newly induced tertiary dentin (*) along and within the pulp chamber. Scale bar, 200 µm. In µCT images, bright radio-opacities represent filling material and surgical debris within the pulp. (**C**) Histological assessment of LPL-treated and control rat teeth with Azan Blue (left panels) and Masson's Trichrome staining (right panels) for tertiary dentin (*) induction. Scale bars, 200 µm.

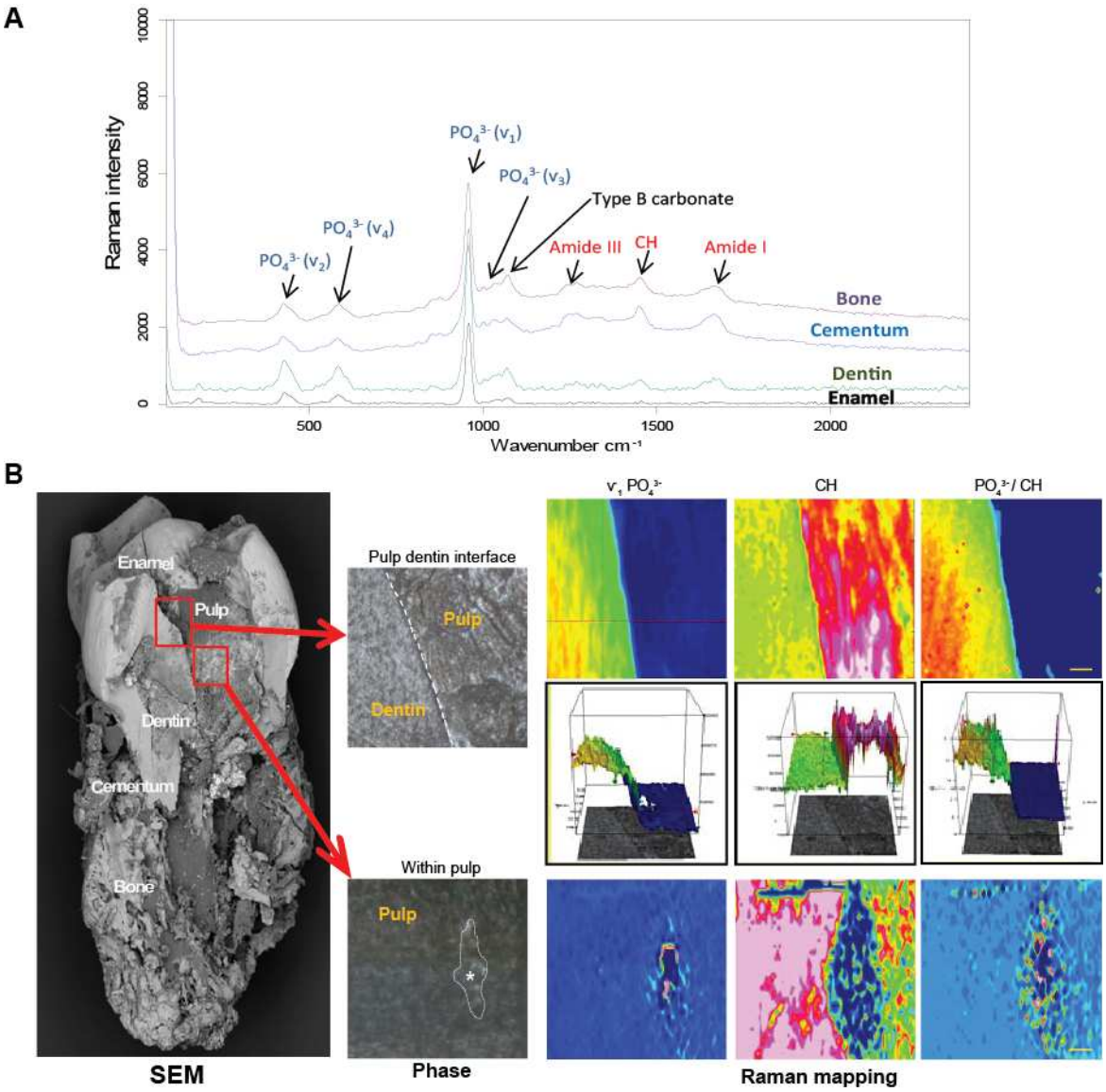

Fig. S2. Raman mapping for compositional assessment of tooth mineralized tissue. (**A**) Raman signatures of mineralized tissues enamel, dentin, cementum, and bone with specific peaks representing compositional elements. (**B**) The large left panel shows a wide-field SEM image of the non-decalcified tooth specimen and the two offset panels show phase images of processed specimens used for Raman imaging (pseudocolored images). Top panels show the v1 PO_4^{3-} (960 cm^{-1}) and CH (1413 cm^{-1}) peaks and their ratio at the pulp-dentin interface. Middle panel shows the spatial distributions of the compositional elements along the tooth structure. Lower panels shows analyses performed within the pulp in calcium hydroxide–treated teeth to identify tertiary dentin induction (*), usually seen as pulp stone-like islands within pulp or along pulpal walls. These distinct, isolated areas were specifically chosen for compositional analyses of tertiary dentin as they permitted clear delineation of the newly formed tertiary dentin from adjacent normal dentin. Scale bars, 100 µm.

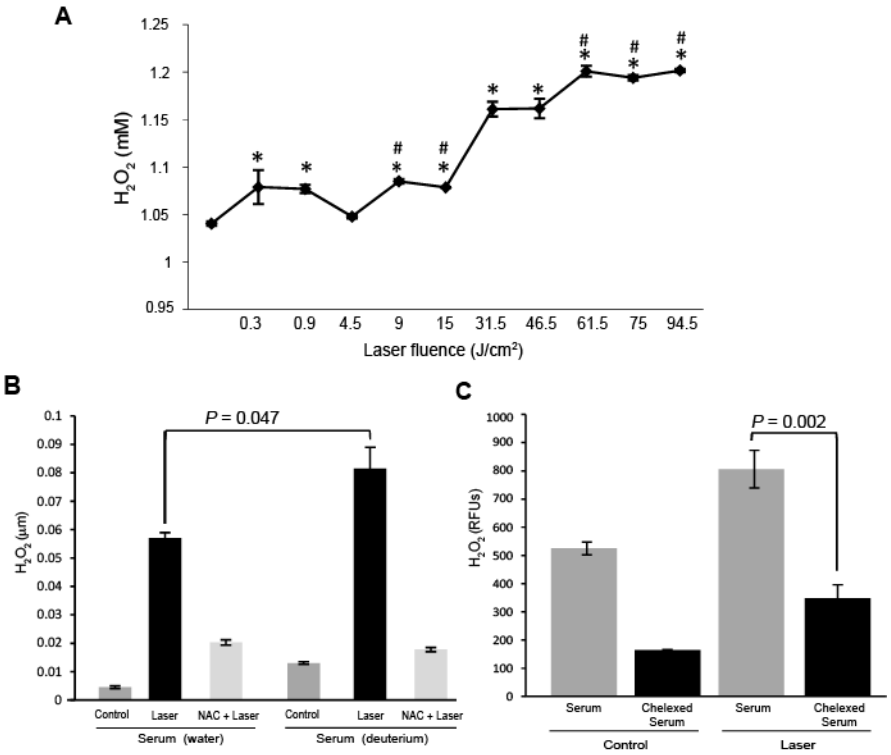

Fig. S3. LPL-generated ROS in a cell-free system. (**A**) H_2O_2 in serum increased following LPL treatment, as assessed with Amplex UltraRed. Fluence (J/cm^2) was varied by changing irradiance (W/cm^2) while keeping distance and treatment time constant. Data are means ± SD (n=3). *P<0.05, two-tailed, t test; $^{\#}P$<0.005, Bonferroni correction for multiple comparisons; data compared to untreated control (first data point). (**B**) Serum diluted with water or deuterium was subjected to LPL (3 J/cm^2) treatment and H_2O_2 generation was assessed with Amplex UltraRed. Some samples were pre-incubated with NAC. (**C**) Analysis of H_2O_2 in serum with and without Chelex 100 resin–treated, and then with and without LPL (3 J/cm^2) treatment. Data in (B and C) are means ± SD (n=3), two-tailed t test. To determine P values, LPL-treated samples were compared in (B) to deuterium- and water-diluted serum samples, and in (C) to Chelex versus non-Chelex treated serum samples.

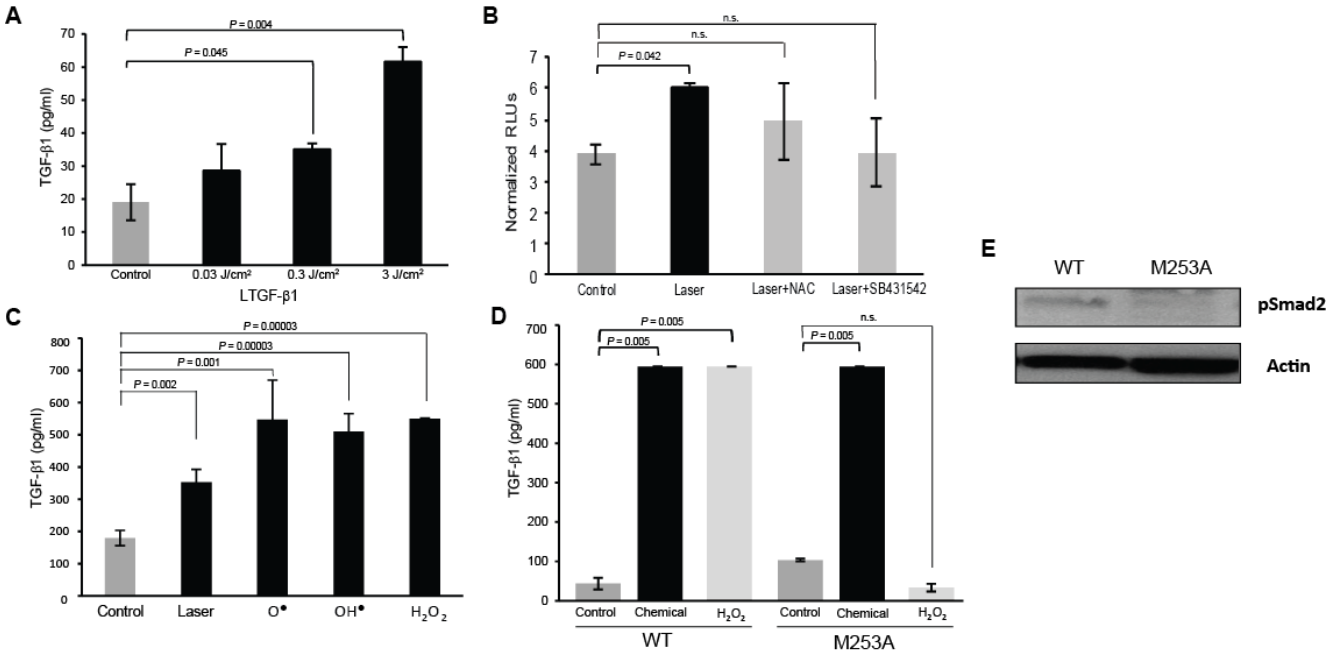

Fig. S4. LPL activation of LTGF-β1 is mediated by ROS. (A) Recombinant latent human TGF-β1 was activated in PBS following LPL treatment in a dose-dependent manner, as assessed with an ELISA. (**B**) Biological activity of LPL-activated TGF-β1, determined using a p3TP-Luc reporter assay. Mv1Lu cells were treated with LPL at 3 J/cm^2 and assessed after 24 h for luciferase activity. Some samples were pre-incubated with NAC (ROS scavenger) or SB431542 (TGF-βRI inhibitor). (**C**) Active TGF-β1 in serum following LPL treatment or after treatments of serum with distinctly generated ROS (table S1) that were also generated by LPL treatments (Fig. 2). (**D**) TGF-β1 in conditioned media from wild type (WT) and ROS-insensitive mutant (M253A) LTGF-β1–transfected MEFs exposed to routine chemical treatment (chemical) and H_2O_2 treatment (100 μM). (**E**) Western blotting for phosphorylated Smad2 levels in H_2O_2–treated cell-conditioned media from M253A MEFs versus WT MEF conditioned media. Data in (A to D) are means ± SD (n = 3). P values determined by two-tailed, t test compared to the untreated samples (control).

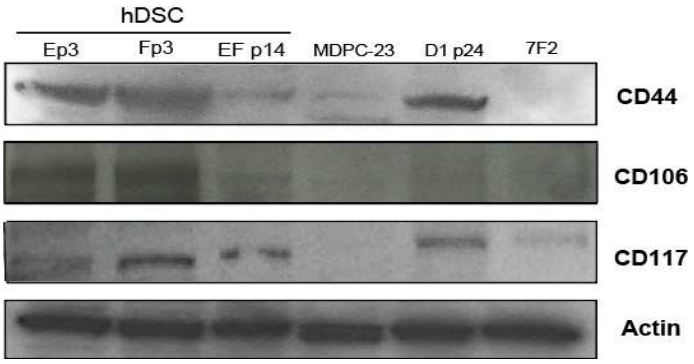

Fig. S5. Characterization of hDSCs. Western blotting for baseline levels of stem cell markers in isolated human dental stem cells (hDSCs). Data is representative of five separate isolations. Cells in culture at passage 3 exhibited a heterogenous morphology, with cells either predominantly epitheloid (Ep3) or fibroblastoid (Fp3) morphology. In later passage, all cells were noted to have the stellate-fibroblastoid morphology, indicated here as EFp14 (at passage 14). For comparison of stem cell surface markers, mouse osteoblast (7F2), mouse pre-odontoblast (MDPC-23), and mouse mesenchymal stem cell (D1) lines were used. In differentiation experiments, hDSCs in passage 3 with the mixed population of epitheloid and fibroblastoid cell morphology were used.

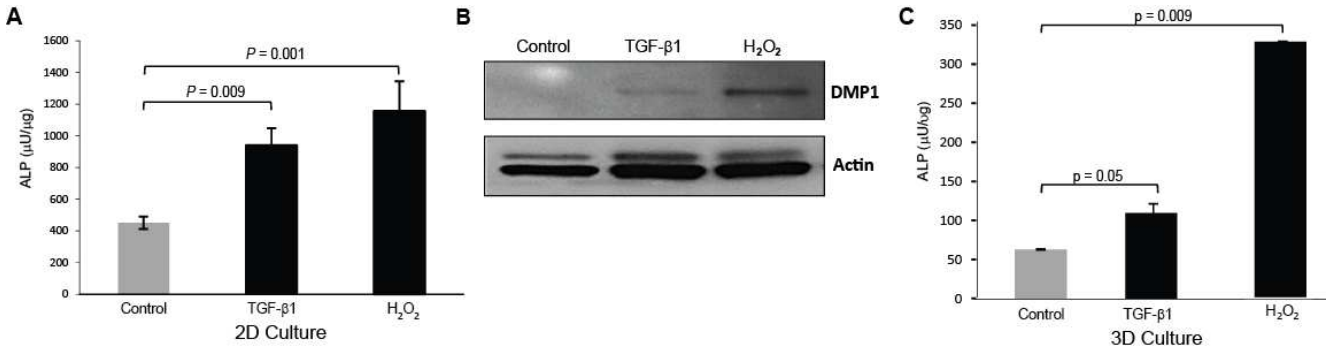

Fig. S6. Culture system for evaluation of the LPL–ROS–TGF-β1 axis. (**A**) Alkaline phosphatase (ALP) activity in MDPC-23 cells in 2D culture in response to TGF-β1 (2.5 ng/ml) or H_2O_2 (100 μM) after 3 days. (**B**) DMP-1 expression in MDPC-23 cells seeded in 3D PLG scaffolds at 21 days in response to TGF-β1 (2.5 ng/ml) or H_2O_2 (100 μM) treatment for 5 min. (**C**) ALP activity in these cell lysates was also assessed. Data in (A and C) are means ± SD (n = 2). P values determined by two-tailed t test.

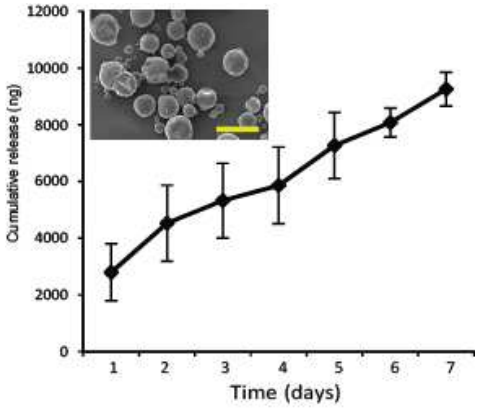

Fig. S7. Release kinetics of TGF-βRI inhibitor from microspheres. Release of TGF-βRI small molecule inhibitor, SB-431542, from PLG microspheres was measured by LC-MS. Data are means ± SD (n = 4). Inset shows SEM images of the microspheres fabricated by the double emulsion technique. Scale bar, 100 µm.

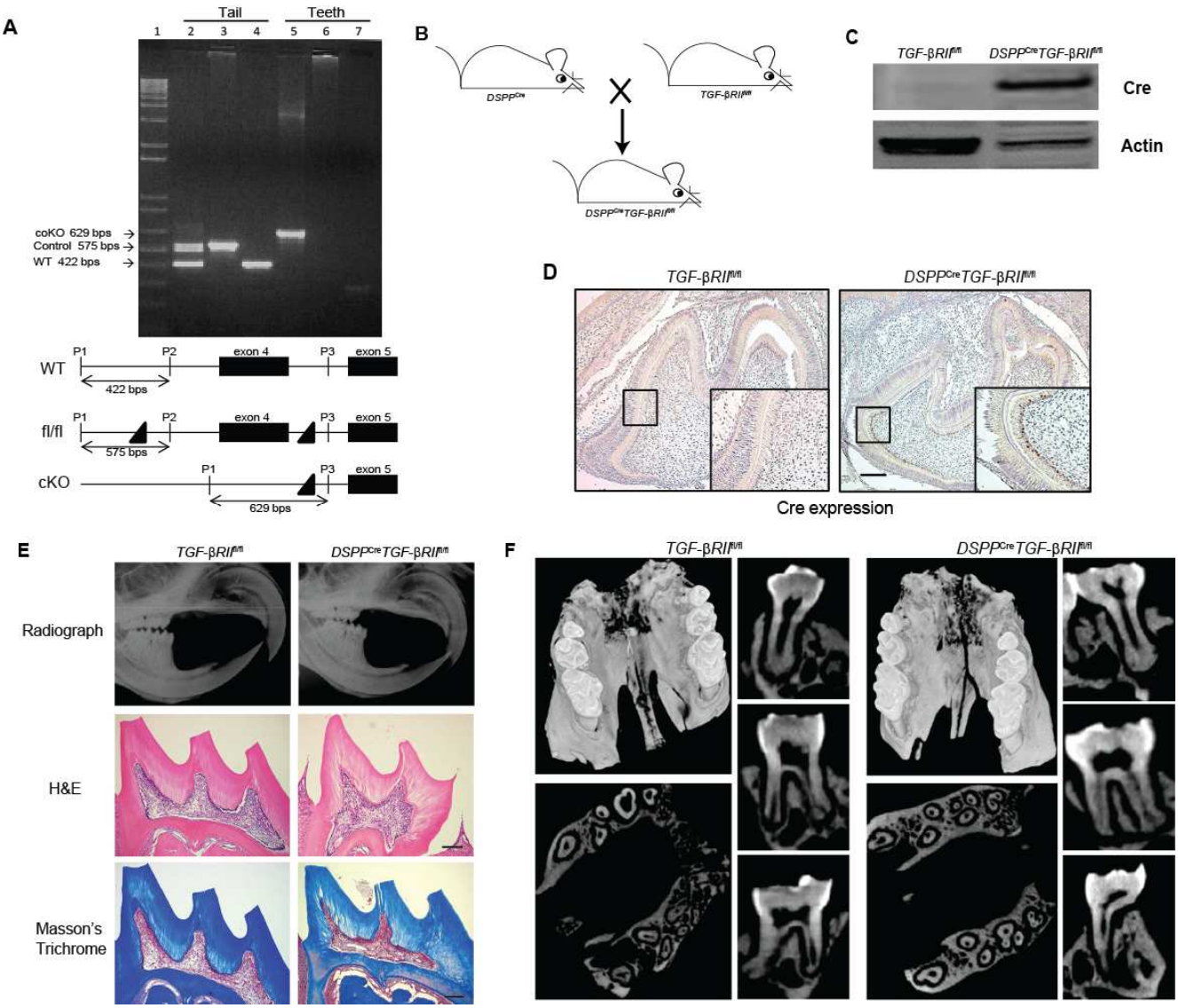

Fig. S8. Characterization of *DSPP*^{Cre}*TGF-*β*RII*$^{fl/fl}$ conditional knockout mice. (**A**) PCR for genotyping was performed with all three primers for genomic tail DNA samples (lanes 2-4) and only primers 1 and 3 for tooth samples (lanes 5-7). (**B**) Strategy for generation of conditional knockout (*DSPP*^{Cre}*TGF-*β*RII*$^{fl/fl}$) mice by crossing *DSPP*^{Cre} with *TGF-*β*RII*$^{fl/fl}$ mice. (**C**) Western blot for Cre expression in teeth from adult transgenic mice. (**D**) Immunostaining for Cre expression in two day–old postnatal teeth in *DSPP*^{Cre}*TGF-*β*RII*$^{fl/fl}$ and *TGF-*β*RII*$^{fl/fl}$ mice. Scale bar, 200 μm. (**E**) Teeth from *TGF-*β*RII*$^{fl/fl}$ and *DSPP*^{Cre}*TGF-*β*RII*$^{fl/fl}$ mice were assessed with radiography, and decalcified sections were examined with H&E and Masson's Trichrome staining. Scale bars, 300 μm (**F**) μCT analyses were performed in maxillary teeth of *TGF-*β*RII*$^{fl/fl}$ and *DSPP*^{Cre}*TGF-*β*RII*$^{fl/fl}$ mice. A gross reconstruction (upper left panels) and a cross-section (lower left panels) are shown. The right panels denote the molar teeth in anterio-posterior (mesiodistal) and sagittal (bucco-lingual) views to assess changes in mineralized tissue volumes and density.

A

B

Mice	Control	Laser
#1	0.773	0.818
#2	0.885	0.923
Mean	0.829	0.873
Standard Deviation	0.079	0.078

Fig. S9. LPL treatment of *TGF*-β*RII*$^{fl/fl}$ wild-type mice. (**A**) Histological assessment of LPL-treated teeth with H&E (left), Toluidine blue (middle), and Masson's Trichrome (right) staining for tertiary dentin (#) induction. Scale bar, 200 µm. (**B**) µCT quantitation performed at 8 weeks to assess tertiary dentin induction in *TGF*-β*RII*$^{fl/fl}$ mice teeth (n = 2).

SUPPLEMENTARY TABLES

Table S1. Reagents used to generate and detect ROS.

ROS*	**Reagents used to generate specific ROS** (concentration)	**Detection method** (concentration)	**Excitation / Emission or Absorbance wavelength (nm)**	**Reagent sources**
Superoxide	Potassium oxide (100 µM) Antimycin A (500 nM)	MitoSOX Red (5 µM)	510 / 580	Sigma, Life Technologies
H_2O_2	H_2O_2 (30% w/w)	Amplex UltraRed (50 µM) CM-H_2DCFDA (10 µM)	560 / 590 490 / 520	Sigma, Life Technologies
Hydroxyl radical	Ferrous perchlorate (100 µM) and H_2O_2 (1 mM)	Proxyl fluorescamine (100 µM)	390 / 480	Sigma, Life Technologies
Nitric oxide	Sodium nitrite (100 mM)	Sulphanilamide (1% w/v) and *N*-1-napthylethylenediamine dihydrochloride (NED) (0.1% w/v)	520	Promega

Note: ROS are extremely reactive and short-lived chemical species. To generate these species as positive controls in our studies, the reagents described above were added to samples. To detect these species, specific probes were used as described in the methods. H_2O_2 is a relatively stable ROS and is available as concentrated solutions. This was used to generate standard curves as well as induce activation in various assays.

Table S2: Primers and conditions for semiquantitative RT-PCR.

Gene	Forward primer(s)	Reverse primer	Method	Reference
DMP1	5′-TCCTTGTGTTCCTTTGGGGG-3′	5′-GGGGTATCTTG GGCACTG TTTTC-3′,	94 - 45 s 60 - 45 s 72 – 45 s x 38 cycles = 341 bps	(*41*)
DSPP	5′-AACAGCAGTGAGGAAAACGGTG-3′	5′-GTGTA AGAAGCATCTCCACGGC -3	94 –30 s 62 – 60 s 72 – 60 s x 36 cycles = 875 bps	(*41*)
OPN	5'-TTGCAG CCTTCTCAGCCAA-3'	5'-CAAAAGCAAATCACTGCAATTCTC-3'	94 – 45 s 60 – 45 s 72 – 45 s x 36 cycles = 146 bps	(*42*)
ALP	5'-ACGT GGCTAAGAATGTCATC-3'	5'-CTGGTAGGCGATGTCCTTA-3',	94-15 s 55-15 s 72-60 s x 38 cycles = 450 bps	(*42*)
GAPDH	5'-ACCA CAGTCCATGCCATCAC-3’	5'-TCCACCACCCTGTTGCTGT-3'	94 – 45 s 60 – 45 s 72 – 45 s x 30 cycles = 500 bps	(*42*)
TGF-βRII	5’- TATGGACT-GGCTTTTGTATTC-3’ and 5’-TGGGGATAGAGGTAGAAAGACATA-3	5-’TATTGGGTGTGGTTGTGGACTTTA-3’	94 – 30 s 62 – 30 s 72 – 45 s x 30 cycles = 422, 575, 692 bps	-----

Table S3: List of antibodies for immunoassays. WB, Western blot; IF, immunofluorescence; IHC, immunohistochemistry.

Antigen	Source	Technique	Dilution	Molecular weights (kDa)
Actin	Chemicon	WB	1:10,000	43
CD106	R&D Systems	WB	1:1000	110
CD117	Cell Signaling	WB	1:1000	120, 140
CD44	Cell Signaling	WB	1:1000	80
CD90	Santa Cruz Biotechnology	IF	1:100	------
Cre	Covance	WB, IHC	1:500, 1:100	39
Dentin matrix protein 1 (DMP1)	Takara	WB	1:1000	37, 57
Osteopontin (OPN)	Hybridoma Bank	WB	1:500	60
Phospho-Smad2	Cell Signaling	WB	1:1000	60
Phospho-Smad2/3	Cell Signaling	IF	1:200	------
Stro-1	Santa Cruz Biotechnology	IF	1:100	------
TGF-β	R&D Systems	WB	1:500	12.5, 25, 105